

Qubit efficient quantum algorithms for the vehicle routing problem on quantum computers of the NISQ era

Ioannis D. Leonidas^{1,3,*}, Alexander Dukakis², Benjamin Tan², and Dimitris G. Angelakis^{1,2,3†}

¹ *School of Electrical and Computer Engineering,
Technical University of Crete, Chania, Greece 73100*

² *Centre for Quantum Technologies, National University of Singapore, 3 Science Drive 2, Singapore 117543 and*

³ *AngelQ Quantum Computing, 531A Upper Cross Street, 04-95 Hong Lim Complex, Singapore 051531*

(Dated: June 16, 2023)

The vehicle routing problem with time windows (VRPTW) is a classic optimization problem that arises in many different areas, such as logistics and transportation. The goal of the VRPTW is to find the shortest possible route for a fleet of vehicles to visit a set of destinations. In recent years, there has been growing interest in using variational quantum algorithms (VQAs), to find approximate solutions to problems that can be formulated as quadratic unconstrained binary optimization (QUBO) problems. In this work, we formulate the VRPTW as a QUBO and apply a quantum variational approach to the VRPTW using our earlier suggested encoding scheme described in [1] to reduce drastically the number of qubits required. We evaluate our approach on a set of VRPTW instances ranging from 11 to 3964 routes constructed with data provided by researchers from Exxon-Mobil. We compare the solutions obtained with standard full encoding approaches for which the max problems size possible in NISQ era are of the order of 20-30 routes. We run our algorithms in simulators as well as cloud quantum hardware provided by IBMQ, AWS (Rigetti) and IonQ and benchmark our results against each other as well as on the simulators. We show that our approach can find approximate solutions to the VRPTW that are comparable to the solutions found by quantum algorithms using the full encoding. Our results suggest that our unique encoding approach, provides a promising approach to drastically reducing the number of qubits required to find decent approximate solutions for industry-based optimization problems.

I. INTRODUCTION

A well studied class of optimization problems is the Quadratic Unconstrained Binary Optimization (QUBO) problems. The importance of QUBO problems stems from the many industry-wide optimization problems that can be re-formulated into QUBO form [1–4], one of which is the vehicle routing problem [5–7]. Finding optimal ways to send vehicles on the shortest routes not only saves a company fuel cost while maximizing their available resources (e.g. number of available vehicles), but is also able to bring a positive impact to our environment due to the decreased carbon footprint of an operation [8–10].

Finding optimal solutions to QUBO problems remain a challenge due to their NP-hard complexity [11]. For a typical industrial application, the vehicle routing problem involves numerous vehicles with possible routes, and enumerating through all possible solutions to find the optimal one is computationally unfeasible. Recent advances in quantum computing have allowed for tools to be developed allowing quantum computers to solve these classical binary optimization problems. Quantum annealing [12] and variational methods such as the Quantum Approximate Optimization Algorithm (QAOA) [13] are typical algorithms of choice for solving QUBO problems on quan-

tum devices. However, the limited capability of state-of-the-art hardware within the era of Noisy Intermediate Scale Quantum (NISQ) devices poses a challenge when applying quantum algorithms to problem sizes typical of applied industry problems [14–16]. These traditional approaches require as many qubits as there are classical variables, making it unfeasible to solve industry problems of any meaningful size.

Using the encoding scheme outlined in [17], classical binary optimization problems involving n_c classical variables can now be solved with up to $\mathcal{O}(\log n_c)$ qubits using gate based quantum devices by using a different method of mapping the qubits to the binary variables. This reduction in qubits needed means quantum devices now have the potential to solve, larger industry-scale QUBO problems, therefore paving the way for industrial applications on NISQ devices.

In this work, we applied the encoding scheme listed in [17] to solve a Vehicle Routing Problem with Time Windows (VRPTW). We compared the solutions obtained from solving an 8 and 11 route instance with the traditional encoding using a similar variational circuit and with the classical commercial solver Gurobi [18]. Following that, we used the encoding scheme from [17] to find solutions to problem instances involving 128 and 3964 routes. Using traditional quantum approaches to find solutions to the 3964 route problem will require more qubits than is currently available if traditional quantum approaches were used instead.

*leonidas@tuc.gr

†dimitris.angelakis@gmail.com

II. VEHICLE ROUTING PROBLEM WITH TIME WINDOWS

Vehicle Routing Problems (VRP) are a well explored and widely applicable family of problems within logistics and operations and are a generalized form of the well-known Travelling Salesman Problem (TSP) [19]. The overarching goal of these problems is to manage and dispatch a fleet of vehicles to complete a set of deliveries or service customers while trying to minimize a total cost. Many variations of this problem exist, oftentimes seeking to maximize profits or minimize travel costs [8, 20].

The Vehicle Routing Problem with Time Windows (VRPTW) is a VRP variant that enforces time windows within which individual deliveries must be made [21–23]. This paper follows the route-based formulation of the VRPTW outlined in [2]. A problem instance is characterized by a network of nodes \mathcal{N} . This set consists of N nodes representing different customers and an additional $0th$ node, d to serve as the "depot" node, which must be the initial departure point and final destination for all vehicles $v \in \mathcal{V}$. Nodes are connected by directed arcs, $(i, j) \in \mathcal{E}$, each of which has an associated cost c_{ij} . These costs are frequently functions of the travel distance or travel time between two nodes, but other measures can also be used. The problem may be specified further by assigning each non-depot node a demand level. For the sake of our work, all vehicles are assumed to be homogeneous both in speed and capacity.

Each node i has an associated time window $[a_i, b_i]$ and can only be serviced after time a_i and before time b_i (although we may permit vehicles to arrive earlier and wait until a_i). The depot can be treated as having a time window of $[0, +\infty]$.

According to this route-based formulation, valid solutions to the problem instance will inform whether or not a route should be travelled. We define a route r as an ordered sequence of P nodes (i_1, i_2, \dots, i_P) for a vehicle to travel to. To satisfy the requirement that vehicles must start and end at the depot, we require that $i_1 = i_P = d$. In order for a route to be considered valid, it must be composed entirely of valid segments: $(i_p, i_{p+1}) \in \mathcal{E} \forall 1 \leq p \leq P - 1$.

We must also ensure that the arrival time T_{i_p} for any given node p along route i , must not exceed the upper limit of that node's time window, i.e. $T_{i_p} \leq b_{i_p} \forall p$. This set \mathcal{R} containing all valid routes defines the size of the problem. For a route $r \in \mathcal{R}$ with sequence (i_1, i_2, \dots, i_P) , we can calculate a route cost $c_r = \sum_{p=1}^{P-1} c_{i_p, i_{p+1}}$. We also define a value $\delta_{i,r}$ which is equal to 1 if node i lies in route r and 0 otherwise. This allows us to express the objective of our VRPTW in terms of a vector \vec{x} , containing decision variables x_r corresponding to each route r :

$$\min_x \sum_r^R c_r x_r, \quad x_r \in \{0, 1\} \forall r \in \mathcal{R} \quad (1)$$

$$\text{s.t.} \sum_r^R \delta_{ir} x_r = 1, \quad \forall i \in \mathcal{N} \quad (2)$$

where x_r is a binary variable that has value 1 if route r is to be travelled, and 0 if not. The linear equality constraint (2) ensures that all nodes in our graph are visited exactly once within our optimal solution.

As an additional optional constraint, it may be desirable to set the number of used vehicles to some fixed value V . This is achieved with the additional condition:

$$\sum_r^R \delta_{0r} x_r = V, \quad (3)$$

where we have used the nomenclature of $\delta_{0,r}$ referring to the inclusion of the depot node in route r . This is included purely for illustrative purposes, as all valid routes must include the depot node and therefore $\delta_{0,r} = 1 \forall r \in \mathcal{R}$.

III. QUADRATIC UNCONSTRAINED BINARY OPTIMIZATION

The QUBO problem is a binary optimization problem consisting of finding a binary vector \vec{x}^* such that:

$$\vec{x}^* = \underset{\vec{x}}{\text{argmin}} \vec{x}^\top \mathcal{A} \vec{x} \quad (4)$$

where $\vec{x} \in \{0, 1\}^{n_c}$ is a vector of n_c classical binary variables and $\mathcal{A}^{n_c \times n_c}$ is a real and symmetric matrix constructed from our optimization problem. Classical methods of finding solutions to the QUBO problem is typically achieved with a range of metaheuristic approximation algorithms such as simulated annealing [24], TABU search [25] or genetic algorithms [26].

To find solutions to the QUBO problem using traditional quantum approaches, the cost function is first mapped to an Ising Hamiltonian:

$$\hat{H}_{\text{Ising}} = \frac{1}{4} \sum_{k,l}^{n_c} \mathcal{A}_{kl} (1 - \hat{\sigma}_z^{(k)}) (1 - \hat{\sigma}_z^{(l)}) \quad (5)$$

where $\hat{\sigma}_z^{(k)}$ is the Pauli z matrix acting on qubit k , and \mathcal{A}_{kj} are the elements of the matrix \mathcal{A} . The ground state of \hat{H}_{Ising} is a basis state $|\vec{x}\rangle$ that corresponds to an exact solution \vec{x} of the QUBO problem defined by \mathcal{A} .

Traditional implementations of VQAs to search for this ground state maps each binary variable in \vec{x} to a single qubit, using the same number of qubits as classical variables i.e. $n_q = n_c$. The resulting quantum state is parameterized by a set of angles $\vec{\theta}$ and can be expressed as a

linear superposition of each basis states $|x_k\rangle$ representing classical solutions \vec{x}_k :

$$|\psi_c(\vec{\theta})\rangle = \hat{U}_c(\vec{\theta})|\psi_0\rangle = \sum_{k=1}^{2^{n_c}} \alpha_k(\vec{\theta})|x_k\rangle, \quad (6)$$

where $\hat{U}_c(\vec{\theta})$ is the unitary evolution implemented on the quantum computer. Classically, the cost function for our QUBO problem when minimizing the energy of \hat{H}_{Ising} can be expressed as:

$$\min C_x = \sum_{k=1}^{2^{n_c}} \vec{x}_k^\top \mathcal{A} \vec{x}_k P(\vec{x}_k). \quad (7)$$

$P(\vec{x}_k)$ is the probability of sampling the classical solution \vec{x}_k . From the quantum state given in (6), this probability of sampling the k^{th} solution is given by the $|\alpha_k(\vec{\theta})|^2$.

In section VI, we describe how the VRPTW formulation as described in II can be mapped into a QUBO problem of the form given in (4).

IV. QUANTUM ALGORITHMS FOR QUBO

A. Quantum Annealing

Quantum annealing is a commonly employed method of solving combinatorial optimization problems using quantum hardware [12]. This method starts by having the qubits in the ground state of a Hamiltonian that can be easily prepared, typically $H_0 = \sum_i^{n_c} \sigma_x^{(i)}$. The system is then evolved slowly towards the Hamiltonian that represents the problem. By the adiabatic theorem, the quantum system will arrive in the ground state of the problem Hamiltonian if the evolution is sufficiently slow [27], and a measurement on the qubits will return the state that minimizes the cost function of the optimization problem at hand. The total Hamiltonian of the system can be expressed as

$$\hat{H} = A(t) \hat{H}_0 + B(t) \hat{H}_{\text{Ising}} \quad (8)$$

where $A(t)$ and $B(t)$ are functions based off the annealing schedule. $A(0) = 1$ and $B(0) = 0$ at the start of the annealing procedure and $A(t_e) = 0$ and $B(t_e) = 1$ at the end of the annealing schedule t_e .

B. Variational hybrid quantum-classical algorithms

Other quantum approaches to solving QUBO problems also include variational methods such as QAOA [13, 28, 29] and hardware efficient parameterized quantum circuits [30, 31]. These approaches involve applying

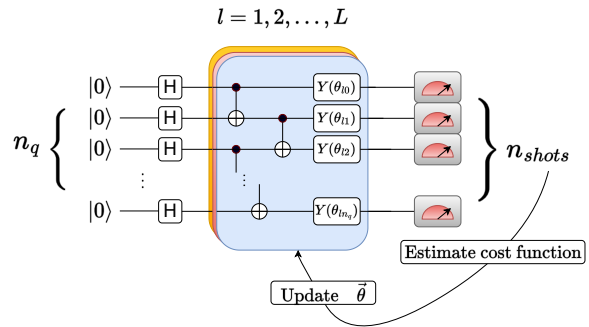


FIG. 1: Hardware efficient variational ansatz for all encoding schemes described. Each circuit begins with a layer of Hadamard gates followed by L repetitions of CNOT gates and single qubit $Y(\theta_i)$ rotations. The circuit is measured in the computational basis to estimate the respective cost functions, and a classical optimizer is used to update the variational parameters $\vec{\theta}$.

some unitary operator $U(\vec{\theta})$ onto some initial quantum state $|\psi_0\rangle$ and using a classical optimizer to adjust the variational parameters $\vec{\theta}$ to find the optimal quantum state $|\psi_{\text{opt}}\rangle = U(\vec{\theta}_{\text{opt}})|\psi_0\rangle$.

In the QAOA, this unitary takes on the following form where P is the number of alternating layers of $U_H(\gamma) = e^{-i\gamma\hat{H}_{\text{Ising}}}$ and $U_x(\beta) = e^{-i\beta\sum\hat{\sigma}_x}$ that are applied to an initial quantum state $|\psi_0\rangle = |+\rangle$ to give

$$|\psi(\vec{\gamma}, \vec{\beta})\rangle = \prod_p^P U_x(\beta_p) U_H(\gamma_p) |+\rangle. \quad (9)$$

The optimal quantum state is found by adjusting the variational parameters $\vec{\gamma} = [\gamma_1, \dots, \gamma_P]$ and $\vec{\beta} = [\beta_1, \dots, \beta_P]$ using classical optimization techniques. QAOA, being a trotterization of the annealing procedure into multiple unitaries, is able to provably converge to the optimal solution as $P \rightarrow \infty$ [13]. However, implementing the QAOA on gate based quantum hardware typically requires deep circuits [32].

In hardware efficient variational approaches, $U(\vec{\theta})$ is constructed using gates that can be efficiently implemented on the specific quantum device available, such as single qubit rotations and two-qubit entangling gates. While easily implemented on quantum hardware, hardware efficient variational approaches typically do not guarantee any convergence to the optimal solution, and suffer from barren plateaus within the cost function landscape, making it difficult to obtain the optimal solution [33–35].

C. Quantum assisted hybrid algorithms

Quantum assisted solvers [36, 37] were recently introduced as a means of solving ground state problems to

Hamiltonians of the form $H = \sum_{i=1}^n \beta_i U_i$ without using a classical-quantum feedback loop. A set of efficiently implementable unitaries V_j is chosen to prepare states $|\phi_j\rangle = V_j|0\rangle$ used in constructing an ansatz of the form

$$|\psi(\vec{\alpha})\rangle = \sum_{j=1}^m \alpha_j |\phi_j\rangle = \sum_{j=1}^m \alpha_j V_j |0\rangle \quad (10)$$

where $\vec{\alpha}$ is a vector of complex values. Once the ansatz is constructed, a quantum computer is used to calculate the overlap matrices $D_{jk} = \sum_i \beta_i \langle \phi_j | U_i | \phi_k \rangle$ and $E_{jk} = \langle \phi_j | \phi_k \rangle$.

To find the optimal values of $\vec{\alpha}$, the following quadratic optimization problem can be solved classically,

$$\text{minimize } \vec{\alpha}^T D \vec{\alpha} \quad (11)$$

$$\text{subject to } \vec{\alpha}^T E \vec{\alpha} = 1 \quad (12)$$

where D , E are matrices constructed using D_{jk} , E_{jk} and written in compact form.

The methods discussed above require mapping a qubit to each binary variable. This requirement limits the use of traditional variational approaches when attempting to solve an industry scale problem on NISQ hardware. In the following section, we will outline how the encoding scheme in [17] can be used to reduce the number of qubits required for a hardware efficient variational approach which can then be applied to the VRPTW problem.

V. SYSTEMATIC ENCODING OF BINARY VARIABLES

The encoding scheme in [17] starts off by dividing the n_c classical variables within the QUBO problem into subgroups of n_a variables. n_a qubits are then used to represent the values of the binary variables within those subgroups, and the basis states of $n_r = \log_2(\frac{n_c}{n_a})$ register qubits are used as addresses to denote which subgroup should take on the values that the ancilla qubits represent. The smallest possible subgroup allowed consists of only one classical variable per subgroup where $n_a = 1$. We refer to this grouping as the *minimal encoding*. The largest possible subgroup allowed is when the subgroup consists of all the classical variables, i.e. $n_a = n_c$, in which case only one possible subgroup exists and no register qubits are needed i.e. $n_q = n_a = n_c$. We refer to this as the *full encoding* and is the one-to-one qubit to variable mapping typically used in the standard approaches described above.

A. Minimal Encoding

The parametrized quantum state can be expressed as

$$|\psi_{\text{me}}(\vec{\theta})\rangle = \sum_{k=1}^{n_c} \beta_k(\vec{\theta}) [a_k(\vec{\theta})|0\rangle_a + b_k(\vec{\theta})|1\rangle_a] \otimes |\phi_k\rangle_r \quad (13)$$

where $\{|0\rangle_a, |1\rangle_a\}$ refer to the quantum state of the $n_a = 1$ qubit and $\{|\phi_k\rangle_r\}$ refer to the quantum state of the register qubits. The cost function for the minimal encoding is the same as (7). However, the probability $P(\vec{x}_i)$ of obtaining a particular bitstring \vec{x}_i is now calculated differently using the state given in (13).

From this state, the probability of the k^{th} binary variable to take on the values 0 and 1 are $P(x_k = 0) = |a_k(\vec{\theta})|^2$ and $P(x_k = 1) = |b_k(\vec{\theta})|^2$ respectively. This gives the total probability $P(\vec{x}_i)$ of obtaining a particular bitstring \vec{x}_i by

$$P(\vec{x}_i) = \prod_{k=1}^{n_c} P(x_k) \quad (14)$$

The minimal encoding allows us to reduce the number of qubits required for a problem with n_c classical variables to $n_q = 1 + \log_2(n_c)$ qubits, the largest reduction possible using the encoding scheme.

By using (14) as our probability distribution in (7) and replacing the probabilities with projectors on our minimal encoding quantum state (13), we obtain the minimal encoding cost function as described in [17]:

$$C_{\text{me}}(\vec{\theta}) = \sum_{k \neq l}^{n_c} A_{kl} \frac{\langle \hat{P}_k^1 \rangle_{\vec{\theta}} \langle \hat{P}_l^1 \rangle_{\vec{\theta}}}{\langle \hat{P}_k \rangle_{\vec{\theta}} \langle \hat{P}_l \rangle_{\vec{\theta}}} + \sum_{k=1}^{n_c} A_{kk} \frac{\langle \hat{P}_k^1 \rangle_{\vec{\theta}}}{\langle \hat{P}_k \rangle_{\vec{\theta}}}, \quad (15)$$

where $\hat{P}_k = |\phi_k\rangle\langle\phi_k|_r$ are projectors over the register basis states $|\phi_k\rangle_r$ and $\hat{P}_k^1 = |1\rangle\langle 1|_a \otimes \hat{P}_k$ are projectors over the states where the ancilla is in the $|1\rangle_a$ state. We emphasize that finding the optimal quantum state in the minimal encoding that minimizes (15) will unambiguously correspond to the classical solution that minimizes the classical QUBO problem in (4).

To obtain a classical bitstring post optimization, coefficients of the optimal quantum state $|\psi_{\text{me}}(\vec{\theta}_{\text{opt}})\rangle$ are obtained by sampling the output of the quantum device, giving us the coefficients $b_k(\vec{\theta}_{\text{opt}})$ as expressed in (13). The probability for the k^{th} bit to be 1 can be calculated via $P(x_k = 1) = |b_k|^2$ (and conversely, $P(x_k = 0) = 1 - |b_k|^2$), and classical solutions can then be sampled according to the probabilities for each bit to be 0 or 1 as described by the final quantum state.

Using a finite number of shots to estimate (15) may result in a division by zero, especially if insufficient shots are used, due to the register states $\langle \hat{P}_k \rangle_{\vec{\theta}}$ not being measured in the denominator. In such cases, the value $\frac{\langle \hat{P}_k^1 \rangle_{\vec{\theta}}}{\langle \hat{P}_k \rangle_{\vec{\theta}}}$

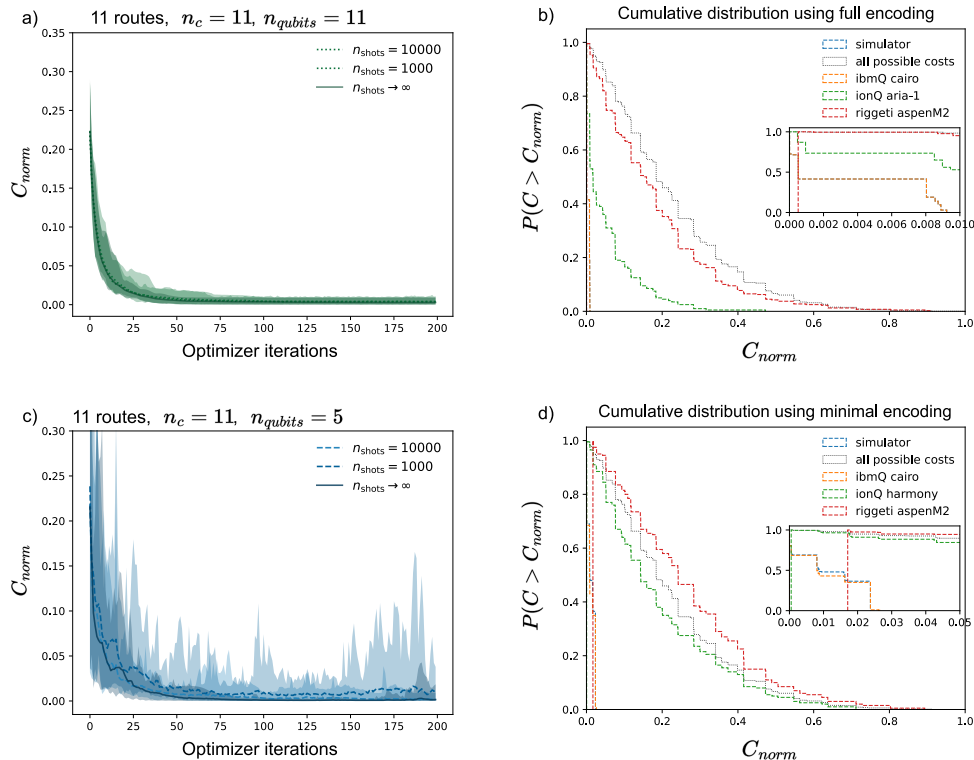


FIG. 2: Comparison between a $n_c = 11$ route optimization instance, using full encoding (top row) and minimal encoding (bottom row). a, c) Convergence graphs for the full encoding and minimal encoding schemes with $n_{\text{meas}} = 1000, 10000$, and $n_{\text{meas}} \rightarrow \infty$. Shaded regions show the deviation of the normalized cost function values per optimizer iteration. b, d) Cumulative distribution of classical solutions obtained post optimization using full and minimal encoding respectively. Black curves show the distribution of C_{norm} values of all 2^{n_c} classical solutions. Blue curves show classical bitstrings obtained using $n_{\text{meas}} = 10000$ shots from simulator. Orange, green, and red curves show the classical bitstrings obtained using the optimal parameters from optimization, on IBMQ, IonQ, and on Rigetti quantum backends. Insets show the zoomed version close to $C_{\text{norm}} = 0$.

in (15), and likewise the value of $|b_k|^2$ when sampling classical solutions from the state, is manually set to be 0.5 which can be interpreted as randomly guessing the value of the k^{th} bit to be 0 or 1 with a 50% probability.

B. Full Encoding

Problems solved using the full encoding scheme will have each classical variable mapped to its own qubit. The full encoded quantum state is given in (6) and the cost function calculated according to (7). Each measurement of the circuit results in a basis state that represents a specific bitstring x_i , whose cost can be calculated according to $C_{\text{fe}} = \vec{x}^T \mathcal{A} \vec{x}$.

VI. EXPERIMENTAL PROCEDURE

In this paper, we solve VRPTW instances of $n_c = 11, 16, 128$ and 3964 routes. In the smaller 2 instances, 2 methods of encoding are used - the traditional method of having one variable to one qubit, and the minimal

encoding requiring $\log_2(n_c) + 1$ qubits. For problem sizes $n_c = 128$ and 3964 , only the minimal encoding was used.

A. Instance generation

A particular VRPTW instance is specified with a set of all valid routes \mathcal{R} . For fully connected problems with N nodes, finding the optimal route becomes intractable very quickly, as the number of possible routes is given by $R_{\text{max}} = \sum_{i=1}^N \frac{N!}{(N-i)!}$. In real-world problems, nodes may not always be fully connected and $R \ll R_{\text{max}}$. All instances considered here were generated from a set \mathcal{R} obtained using a greedy heuristic provided in [2].

From this point, we need to convert our set of routes into a QUBO problem of the form in (4). Starting from the cost function of the classical optimization problem in (1), and adding additional penalty terms to represent our constraints, we can arrive at a new, unconstrained cost function:

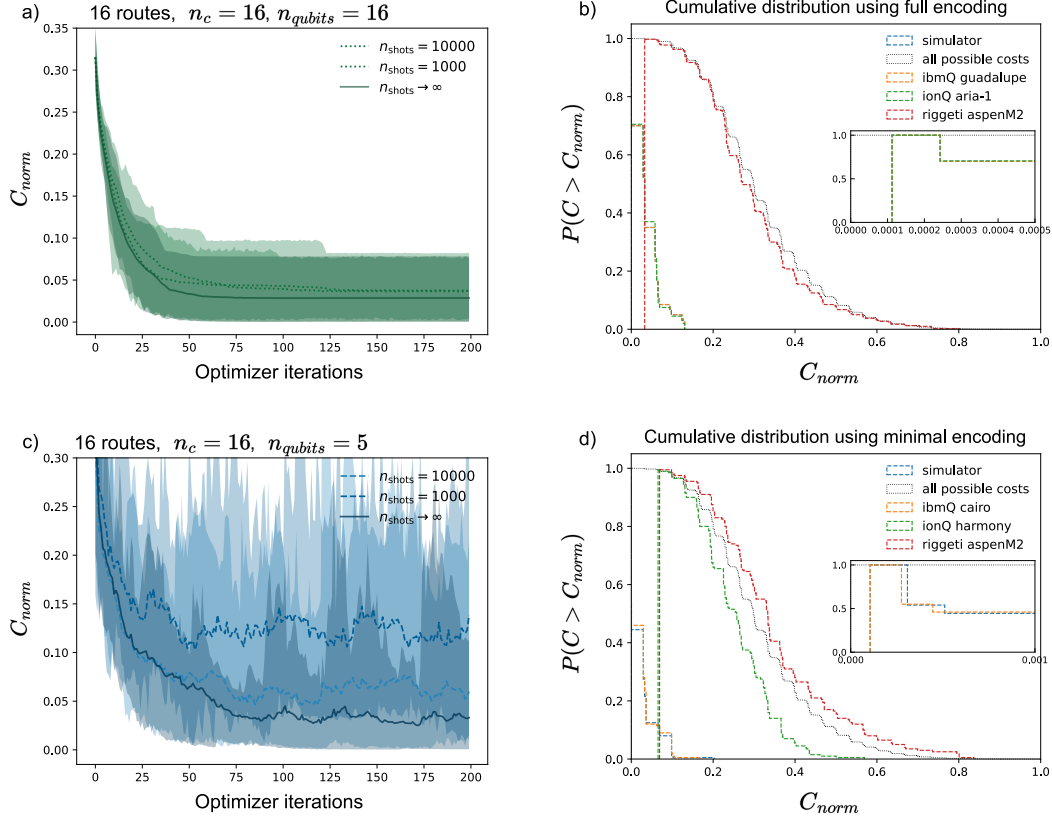


FIG. 3: Comparison between the full encoding and minimal encoding for a $n_c = 16$ route problem, using $n_q = 16$ qubits for the full encoding and $n_q = 5$ qubits for the minimal encoding. a, c) Optimization runs over 20 starting points. Shaded region shows minimum and maximum value of the 20 runs obtained at each optimization iteration. b, d) Cumulative distribution of bitstrings obtained using $n_{meas} = 10000$ shots on a simulator (blue), IBMQ (orange), IonQ (green), Rigetti (red) quantum backends compared with the distribution of all possible cost function values (black). Inset shows zoomed in versions of the cumulative distributions close to $C_{norm} = 0$.

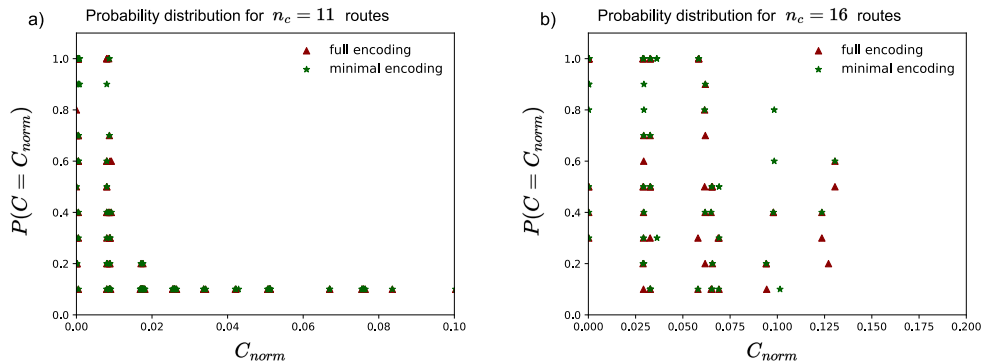


FIG. 4: Probability distribution of solutions obtained with minimal and full encoding for a) 11 routes and b) 16 routes. For each instance, 10 classical bitstrings are sampled from quantum states obtained by IonQ and IBMQ quantum computers. Then all bitstrings are binned according to their cost function values and grouped based on the encoding scheme used to obtain them. We observe that while the minimal encoding can produce approximate solutions of similar quality to the full encoding, it also results in a larger spread of bitstrings sampled.

$$\min_{\vec{x}} \sum_r^R c_r x_r + \rho \sum_i^N \left(\sum_r^R \delta_{ir} x_r - 1 \right)^2. \quad (16)$$

where ρ is a positive penalty coefficient that serves to increase our cost function by an additional amount whenever a constraint is violated i.e. $\sum_r^R \delta_{ir} x_r \neq 1$. Since, in the worst case scenario, we require this penalty to outweigh the maximum total cost, we set $\rho \geq \sum_r^R |c_r|$ [2]. We can expand the squared term and write (16) in the form:

$$\begin{aligned} & \min_{\vec{x}} \sum_r^R c_r x_r \\ & + \rho \sum_i^N \left[\left(\sum_r^R \delta_{ir} x_r \right) \left(\sum_{r'}^R \delta_{ir'} x_{r'} \right) \right. \\ & \left. - 2 \sum_r^R \delta_{ir} x_r + 1 \right] \\ = & \min_{\vec{x}} \sum_r^R c_r x_r + \rho \sum_i^N \sum_r^R \sum_{r'}^R \delta_{ri}^\top x_r x_{r'} \delta_{ir'} \\ & - 2\rho \sum_i^N \left(\sum_r^R \delta_{ir} x_r \right) \\ & + \rho N \end{aligned} \quad (17)$$

Equation (18) can be written in matrix and vector form:

$$\min_{\vec{x}} \vec{c}^\top \vec{x} + \rho \vec{x} \delta^\top \delta \vec{x} - 2\rho \left(\vec{1}^\top \delta \right) \vec{x} + \rho N \quad (19)$$

from which we can identify the quadratic, linear, and constant terms. By setting matrix $\mathcal{A} = \text{diag}(\vec{c}) + \rho \delta^\top \delta - \text{diag}(2\rho \vec{1}^\top \delta)$, where $\text{diag}(\vec{c})$ denotes a matrix with \vec{c} in its diagonal, we arrive at the definition of a QUBO problem in (4).

B. Optimization procedure

Each problem is set up with a basic variational ansatz with $L = 4$ layers of the gates exemplified in [FIG 1] We used ADAM [38], a gradient based classical optimizer, to find the optimal parameters for our circuit. During each iteration, the parameter shift rule [39] was used to calculate the gradient of each parameter. The final parameters were used to run optimal circuits using a noise-free simulator in PennyLane [40] and, depending on the problem sizes, on the cairo, guadalupe, quantum backends from IBMQ [41], the Aspen M2 quantum backend from Rigetti via the AWS Braket [42], and on the harmony and aria-1

quantum backends from IonQ [43]. In all problem instances for both the minimal and full encoding case, 20 randomly seeded starting points, $\vec{\theta}_{\text{init}}$, were used. 10 classical solutions were sampled from the post-optimization quantum state for a total of 200 classical solutions per problem instance, and compared according to a cumulative distribution of their normalized cost function value:

$$C_{\text{norm}} = \frac{(C(\vec{\theta}) - C_{\text{min}})}{(C_{\text{max}} - C_{\text{min}})} \quad (20)$$

where C_{min} and C_{max} are the minimum and maximum cost function values associated with the problem instances, found using Gurobi [18]. Classical solutions were drawn from the minimal encoding quantum state as described in section V.A. In the case of full encoded problems, to obtain the probability distribution of the solutions we simply measure the quantum circuit in the computational basis. By doing so, we are able to compare these two encoding techniques based on the classical solutions obtained from each method and their associated costs for each VRPTW instance.

VII. COMPARISON OF MINIMAL ENCODING WITH FULL ENCODING SCHEME

The optimization run and approximate solutions obtained for the smaller problem sizes of $n_c = 11, 16$ can be seen in [FIG 2] and [FIG 3] respectively. Optimization was done for using different number of shots n_{meas} depending on the size of the problem, and compared with runs completed with full access to the statevector (i.e. $n_{\text{meas}} \rightarrow \infty$). For such small problem sizes, the number of shots required to converge to a solution similar to that obtained using statevector simulation is well within the capabilities of current quantum devices. With sufficient shots to estimate the quantum state, ADAM is able to find solutions of similar quality for both the minimal encoding and the full encoding, despite the minimal encoding requiring fewer qubits. Using the quantum backends, we are able to observe from [FIG 4] approximate solutions sampled from both the minimal and full encoding.

Classical solutions sampled from the full encoded quantum state tended to produce slightly higher quality solutions compared to those sampled from the minimal encoded state. In both the minimal encoding and full encoding case, classical solutions obtained from quantum states produced by the IBMQ quantum backends consistently outperformed those obtained from the IonQ and Rigetti backends. [FIG 2] and [FIG 3] also shows the IonQ devices being able to produce better quality solutions for the full encoded cases compared to solutions sampled from the minimal encoding. However, due to scheduling issues, problem instances requiring fewer qubits (such as those using the minimal encoding) were executed on harmony instead of aria-1 qpu, and further

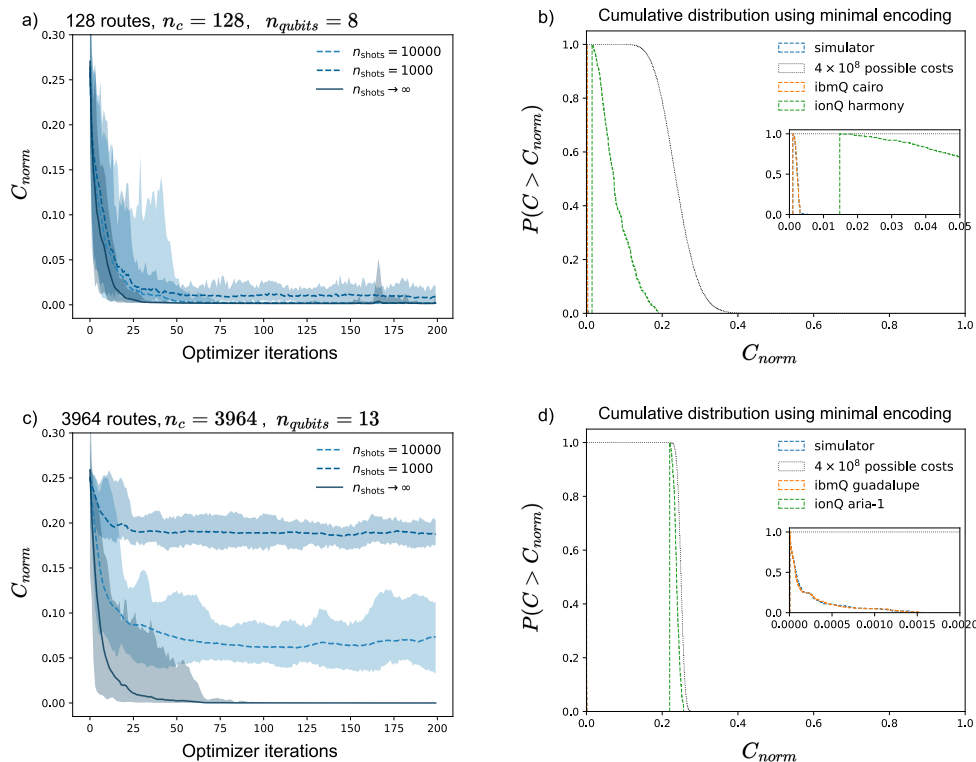


FIG. 5: Optimization runs and cumulative distribution of solutions using minimal encoding for the $n_c = 128$ instance using $n_q = 8$ qubits (top row) and $n_c = 3964$ instance using $n_q = 13$ qubits (bottom row). Black dotted curves represents the cumulative distribution of 4×10^8 randomly generated solutions. Blue, orange, and green curves display the cumulative distribution of solutions obtained using minimal encoding with $n_{meas} = 10000$ shots on a noise free simulation and on IBMQ, IonQ quantum backends respectively.

testing is required to conclude the source of these differences for the IonQ backends.

We observe that the optimization runs using the minimal encoding tend to fluctuate much more compared to runs using the full encoding. We attribute this to the minimal encoding quantum state not being able to fully capture correlations between the classical variables. The cost function for the minimal encoding, C_{me} , as expressed in (15), means that classical bitstrings of n_c length do not need to be reconstructed at each step during the optimization phase. However, the construction of the QUBO problem using data from the VRPTW typically results in large variation in the absolute value of the matrix elements due to the value of ρ in (17), which can be several times the size of c_r , the cost of each route. These large variances in the matrix elements translate greater sensitivity of the cost function, as small adjustments made to any of the coefficients $|a_k(\vec{\theta})|$ and $|b_k(\vec{\theta})|$ in (13) are multiplied with large matrix values. For the case of the full encoding, a change in the probability of sampling a bitstring is spread out over the rest of the basis states, reducing the variance over the range of cost function values.

VIII. FINDING SOLUTIONS TO VRPTW PROBLEMS OF LARGER PROBLEM SIZES

To further push the boundaries on the sizes of industry relevant problems that can be solved on quantum devices, we apply the minimal encoding method to find approximate solutions to VRPTW problems of $n_c = 128$ and $n_c = 3964$ classical variables, using the methods outlined in VI.B with $n_q = 8$ and $n_q = 13$ qubits respectively. While the 128 route instance was able to find decent solutions using similar number of shots as the 11 and 16 route instances, the number of resources required to obtain decent solutions increases significantly for the 3964 route instance, as seen in [Fig 5c] where the number of shots limits the quality of solutions that can be obtained. Solutions obtained using the IBM quantum backends fall within the range of those obtained in noise free simulations, as observed in [Fig 5d], although the exact optimal solution was not found for any of the two bigger problem instances as seen in [Fig 6].

Similar to the results for the smaller problem instances in [FIG 2] and [FIG 3], the solutions obtained from the IBMQ backends were far superior to those obtained from the IonQ devices using the minimal encoding. For a 13 qubit system, a quantum state has $2^{13} = 8192$ ba-

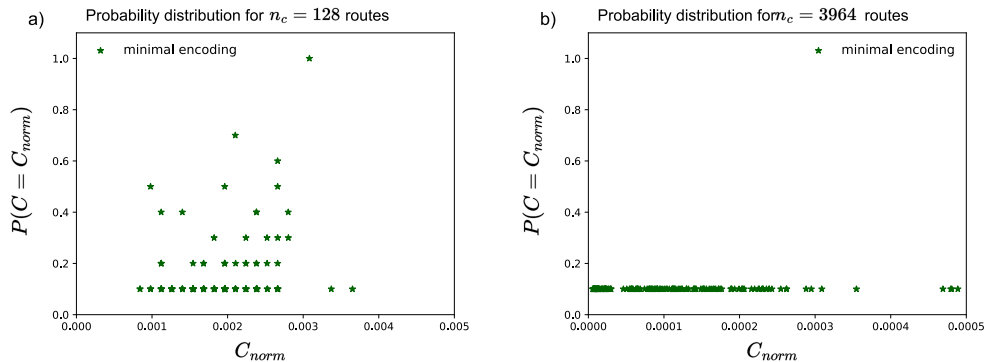


FIG. 6: Probability distribution of solutions obtained with minimal encoding for a) $n_c = 128$ and b) for $n_c = 3964$ classical variables. We calculate these probabilities by using the best variational parameters found from the optimization procedure and sample 10 bitstrings per instance using the IonQ and IBMQ quantum backends. Using $n_q = 11$ and $n_q = 13$ qubits respectively, minimal encoding finds approximate solutions of same quality as the optimal solution as seen from the range of C_{norm} i.e. for $n_q = 13$ approximate solutions are uniformly distributed in $(0, 0.0005)$ of the optimal solution.

sis vectors in the computational basis, and 10,000 shots is insufficient to accurately characterize all coefficients associated with the basis vectors. After expressing each state in the form given in (13), these leave many register states unmeasured, resulting in a large number of binary variables in \vec{x} that have to be guessed, resulting in poor quality solutions overall. For such problem instances, it is expected that more shots would be required, although this was not explored in this work due to cost limitations.

IX. CONCLUSION

In this work, we applied the encoding scheme described in [17] to a common optimization problem faced within the industry, namely the vehicle routing optimization problem. We compared the results obtained from optimization runs using the minimal encoding and the full encoding for problem sizes of 11 routes and 16 routes and classical solutions sampled from the final states prepared on quantum backends offered by IBMQ, IonQ, and Rigetti via the AWS Braket. We pushed the boundaries for problem sizes that can be solved using quantum devices by testing the minimal encoding on problem sizes involving 128 and 3964 routes, and compared the solutions obtained using quantum states prepared by the IBMQ and IonQ quantum devices.

The formulation of the VRPTW as a QUBO results in a cost function spectrum where feasible solutions lie close

together and are separated from infeasible solutions by a large gap. This spectrum can make it more difficult for feasible solutions to be found using the minimal encoding due to the quantum state not being able to capture any classical correlations between the variables, leading to increased variance in the cost function during optimization, and due to the quality of solutions becoming more sensitive to the optimization parameters (e.g. the number of shots).

Our results show that optimization runs using the minimal encoding were still able to find classical solutions of similar quality to runs using the full encoding scheme, despite using much fewer qubits and the limitation of not being able to capture any classical correlations. Future work in this direction to improve performance could include optimizing over the log of the QUBO matrices to reduce variances within the cost function landscape, as well as additional post-processing methods to obtain feasible solutions (solutions which satisfy all the constraints) from infeasible ones. This should allow for approximate valid solutions to still be found despite some of the optimization runs terminating in a local minima where only some of the constraints are satisfied.

Acknowledgments.— We want to thank Dimitar Tenev and Stuart Harwood for his support on formulating the VRPTW instances. We acknowledge support from the National Research Foundation, Prime Minister’s Office, Singapore and A*STAR under its Quantum Engineering Programme (NRF2021-QEP2-02-P02).

-
- [1] Pontus Vikstål, Mattias Grönkvist, Marika Svensson, Martin Andersson, Göran Johansson, and Giulia Ferrini. Applying the quantum approximate optimization algorithm to the tail-assignment problem. *Physical Review Applied*, 14(3):034009, 2020.
- [2] Stuart Harwood, Claudio Gambella, Dimitar Tenev, An-

- drea Simonetto, David Bernal, and Donny Greenberg. Formulating and solving routing problems on quantum computers. *IEEE Transactions on Quantum Engineering*, 2:1–17, 2021.
- [3] G. Kochenberger, J.K. Hao, F. Glover, M. Lewis, Z.P. Lü, H.B Wang, and Y. Wang. The unconstrained binary

- quadratic programming problem: a survey. *Journal of Combinatorial Optimization*, 28(1):58–81, 2014.
- [4] Fred Glover, Gary Kochenberger, and Yu Du. A tutorial on formulating and using qubo models. *arXiv preprint arXiv:1811.11538*, 2018.
- [5] George B Dantzig and John H Ramser. The truck dispatching problem. *Management science*, 6(1):80–91, 1959.
- [6] Kris Braekers, Katrien Ramaekers, and Inneke Van Nieuwenhuysse. The vehicle routing problem: State of the art classification and review. *Computers & industrial engineering*, 99:300–313, 2016.
- [7] Paolo Toth and Daniele Vigo. *The vehicle routing problem*. SIAM, 2002.
- [8] Canhong Lin, King Lun Choy, George TS Ho, Sai Ho Chung, and HY Lam. Survey of green vehicle routing problem: past and future trends. *Expert systems with applications*, 41(4):1118–1138, 2014.
- [9] Reza Moghdani, Khodakaram Salimifard, Emrah Demir, and Abdelkader Benyettou. The green vehicle routing problem: A systematic literature review. *Journal of Cleaner Production*, 279:123691, 2021.
- [10] Imdat Kara, Bahar Y Kara, and M Kadri Yetis. Energy minimizing vehicle routing problem. In *Combinatorial Optimization and Applications: First International Conference, COCOA 2007, Xi'an, China, August 14-16, 2007. Proceedings 1*, pages 62–71. Springer, 2007.
- [11] F Barahona. On the computational complexity of ising spin glass models. *Journal of Physics A: Mathematical and General*, 15(10):3241, oct 1982.
- [12] Wolfgang Lechner, Philipp Hauke, and Peter Zoller. A quantum annealing architecture with all-to-all connectivity from local interactions. *Science Advances*, 1(9):1–6, 2015.
- [13] Edward Farhi, Jeffrey Goldstone, and Sam Gutmann. A quantum approximate optimization algorithm. *arXiv preprint arXiv:1411.4028*, 2014.
- [14] John Preskill. Quantum Computing in the NISQ era and beyond. *Quantum*, 2:79, August 2018.
- [15] Frank Leymann and Johanna Barzen. The bitter truth about gate-based quantum algorithms in the nisq era. *Quantum Science and Technology*, 5(4):044007, 2020.
- [16] Jonathan Wei Zhong Lau, Kian Hwee Lim, Harshank Shrotriya, and Leong Chuan Kwek. Nisq computing: where are we and where do we go? *AAPPS Bulletin*, 32(1):27, 2022.
- [17] Benjamin Tan, Marc-Antoine Lemonde, Supanut Thanasilp, Jirawat Tangpanitanon, and Dimitris G. Angelakis. Qubit-efficient encoding schemes for binary optimisation problems. *Quantum*, 5:454, may 2021.
- [18] LLC Gurobi Optimization. Gurobi optimizer reference manual, 2020.
- [19] Jan Karel Lenstra and AHG Rinnooy Kan. Some simple applications of the travelling salesman problem. *Journal of the Operational Research Society*, 26(4):717–733, 1975.
- [20] Bezalel Gavish and Stephen C Graves. The travelling salesman problem and related problems, 1978.
- [21] Marius M Solomon and Jacques Desrosiers. Survey paper—time window constrained routing and scheduling problems. *Transportation science*, 22(1):1–13, 1988.
- [22] Marius M Solomon. Algorithms for the vehicle routing and scheduling problems with time window constraints. *Operations research*, 35(2):254–265, 1987.
- [23] Olli Bräysy and Michel Gendreau. Vehicle routing problem with time windows, part i: Route construction and local search algorithms. *Transportation science*, 39(1):104–118, 2005.
- [24] Scott Kirkpatrick, C Daniel Gelatt Jr, and Mario P Vecchi. Optimization by simulated annealing. *science*, 220(4598):671–680, 1983.
- [25] Yang Wang, Zhipeng Lü, Fred Glover, and Jin-Kao Hao. A multilevel algorithm for large unconstrained binary quadratic optimization. In *Integration of AI and OR Techniques in Constraint Programming for Combinatorial Optimization Problems: 9th International Conference, CPAIOR 2012, Nantes, France, May 28–June 1, 2012. Proceedings 9*, pages 395–408. Springer, 2012.
- [26] Siong Thye Goh, Sabrish Gopalakrishnan, Jianyuan Bo, and Hoong Chuin Lau. A hybrid framework using a qubo solver for permutation-based combinatorial optimization. *arXiv preprint arXiv:2009.12767*, 2020.
- [27] Tameem Albash and Daniel A. Lidar. Adiabatic quantum computation. *Rev. Mod. Phys.*, 90:015002, Jan 2018.
- [28] Edward Farhi, Jeffrey Goldstone, and Sam Gutmann. A quantum approximate optimization algorithm applied to a bounded occurrence constraint problem. *arXiv preprint arXiv:1412.6062*, 2014.
- [29] G. Pagano, A. Bapat, P. Becker, K. S. Collins, A. De, P. W. Hess, H. B. Kaplan, A. Kyprianidis, W. L. Tan, C. Baldwin, L. T. Brady, A. Deshpande, F. Liu, S. Jordan, A. V. Gorshkov, and C. Monroe. Quantum approximate optimization of the long-range ising model with a trapped-ion quantum simulator. *arXiv preprint arXiv:1906.02700*, 2019.
- [30] Abhinav Kandala, Antonio Mezzacapo, Kristan Temme, Maika Takita, Markus Brink, Jerry M. Chow, and Jay M. Gambetta. Hardware-efficient variational quantum eigensolver for small molecules and quantum magnets. *Nature*, 549(7671):242–246, 2017.
- [31] Arthur G. Rattew, Shaohan Hu, Marco Pistoia, Richard Chen, and Steve Wood. A domain-agnostic, noise-resistant, hardware-efficient evolutionary variational quantum eigensolver. *arXiv preprint arXiv:1910.09694*, 2019.
- [32] Gereon Kofmann, Lennart Binkowski, Lauritz van Luijk, Timo Ziegler, and René Schwonnek. Deep-circuit qaoa. *arXiv preprint arXiv:2210.12406*, 2022.
- [33] Jarrod R. McClean, Sergio Boixo, Vadim N. Smelyanskiy, Ryan Babbush, and Hartmut Neven. Barren plateaus in quantum neural network training landscapes. *Nature Communications*, 9(1):4812, 2018.
- [34] Marco Cerezo, Akira Sone, Tyler Volkoff, Lukasz Cincio, and Patrick J Coles. Cost function dependent barren plateaus in shallow parametrized quantum circuits. *Nature communications*, 12(1):1–12, 2021.
- [35] Samson Wang, Enrico Fontana, Marco Cerezo, Kunal Sharma, Akira Sone, Lukasz Cincio, and Patrick J Coles. Noise-induced barren plateaus in variational quantum algorithms. *Nature communications*, 12(1):6961, 2021.
- [36] Kishor Bharti. Quantum assisted eigensolver. *arXiv preprint arXiv:2009.11001*, 2020.
- [37] Kishor Bharti and Tobias Haug. Iterative quantum-assisted eigensolver. *Physical Review A*, 104(5):L050401, 2021.
- [38] Zijun Zhang. Improved adam optimizer for deep neural networks. In *2018 IEEE/ACM 26th International Symposium on Quality of Service (IWQoS)*, pages 1–2. Ieee, 2018.

- [39] Gavin E Crooks. Gradients of parameterized quantum gates using the parameter-shift rule and gate decomposition. *arXiv preprint arXiv:1905.13311*, 2019.
- [40] Ville Bergholm, Josh Izaac, Maria Schuld, Christian Gogolin, Carsten Blank, Keri McKiernan, and Nathan Killoran. PennyLane: Automatic differentiation of hybrid quantum-classical computations, 2022.
- [41] IBM Quantum team. Retrieved from <https://quantum.computing.ibm.com>. Ibmq, 2020.
- [42] Amazon Braket. <https://aws.amazon.com/braket/>.
- [43] IonQ Trapped Ion Quantum Computing <https://ionq.com/>.